

Oxidation of Olefins with Benzeneseleninic Anhydride in the Presence of TMSOTf

Izabella Jastrzębska,^{*,†} Maja Morawiak,[‡] Joanna E. Rode,^{‡,§} Barbara Seroka,[†] Leszek Siergiejczyk,[†] and Jacek W. Morzycki^{*,†}

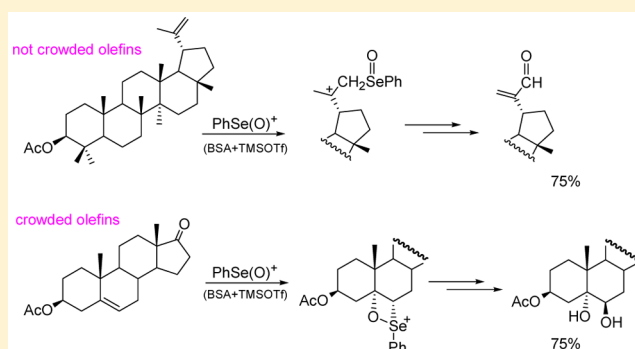
[†]Institute of Chemistry, University of Białystok, ul. Ciołkowskiego 1K, 15-245 Białystok, Poland

[‡]Institute of Organic Chemistry, Polish Academy of Sciences, ul. Kasprzaka 44, 01-224 Warsaw, Poland

[§]Institute of Nuclear Chemistry and Technology, ul. Dorodna 16, 03-195 Warsaw, Poland

Supporting Information

ABSTRACT: A new oxidizing system for olefins, consisting of benzeneseleninic anhydride and trimethylsilyl triflate, was studied. The highly reactive benzeneseleninyl cation is presumably formed under these conditions. It has been shown that different products are formed with this species depending on the specific structure of olefin. The 1,1-disubstituted olefins afforded mostly α,β -unsaturated carbonyl compounds. The sterically encumbered tri- or tetrasubstituted olefins yielded 1,2- or 1,4-dihydroxylated products, presumably via four-membered cyclic intermediates.



INTRODUCTION

Benzeneseleninic anhydride (BSA) is a classical organoselenium reagent frequently used, among other tetravalent selenium compounds, for the oxidation of organic compounds.¹ At first, BSA was mainly used for alcohol oxidation. The reagent was introduced in the late 1970s by Barton et al.² However, BSA oxidation is also a valuable tool for preparation of various oxygenated compounds. For instance, previously reported reactions employing BSA include the oxidation of phenols to hydroxycyclohexadienones³ or *ortho*-quinones,⁴ thiocarbonyl compounds to their corresponding oxo derivatives,⁵ hydrazones and hydroxylamines,⁶ hydrazones, oximes, and semicarbazones to ketones,⁷ and hydrazines to diazenes.⁸ The dehydrogenation reactions of ketones⁹ and lactams,¹⁰ as well as the allylic oxidation of alkenes,¹¹ have also been documented. Furthermore, diphenyl diselenide has been used as a catalytic reagent in the presence of a stoichiometric oxidizing reagent such as di-*tert*-butyl peroxide,¹² iodoxybenzene,¹³ or hydrogen peroxide.¹⁴ Apparently, in these processes, BSA (or benzeneseleninic acid) was formed in situ.¹⁵

In the 1990s, certain efforts were directed toward the use of BSA in the presence of diphenyl diselenide/triflic anhydride.¹⁶ Under these conditions, benzeneselenenyl triflate [PhSe(O)(O)₂CF₃] was generated. The reaction of terminal alkenes with this species produced vicinal areneseelenenyl triflates. Also, olefin oxidation with benzeneseleninyl trifluoroacetate [PhSe(O)OC(O)CF₃], generated in situ from BSA and trifluoroacetic anhydride, was briefly studied.^{16,17} The oxidation of disubstituted olefins with this reagent effectively yielded 2-(phenylseleno)-1,3-alkanediols. The aim of the present study

was to test the effect of trimethylsilyl trifluoromethanesulfonate (TMSOTf) on the oxidation reactions with BSA. Herein, we report a new and effective one-pot method for the oxidation of olefins.

RESULTS AND DISCUSSION

At the beginning, the oxidation of Δ^5 -steroids with BSA/TMSOTf was studied. The reactions were carried out with 1 equiv of BSA and 0.5 equiv of TMSOTf relative to the starting steroidal olefin in dry dichloromethane for 45–60 min [thin-layer chromatography (TLC) control] at room temperature. Surprisingly, the *trans*-dihydroxylation of the double bond occurred during the reaction and afforded 5 α ,6 β -dihydroxy derivatives (1–5) of starting Δ^5 -steroids in good yields (Table 1).

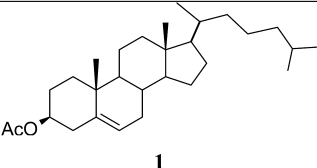
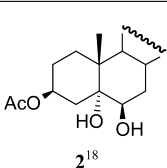
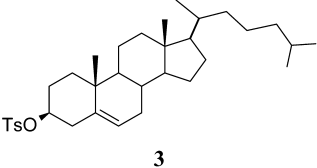
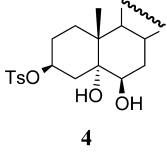
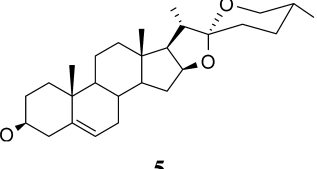
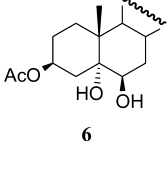
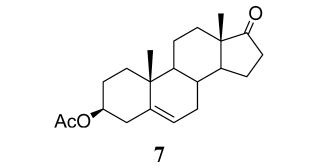
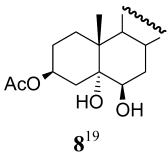
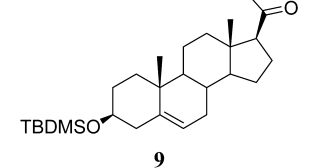
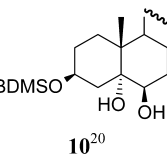
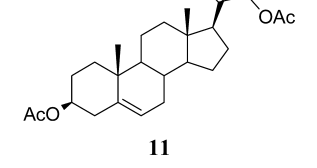
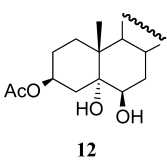
Due to the relatively mild reaction conditions, even sensitive groups such as tosylate, TBDMS, and the spirostane side chain remained intact during the reaction. Steroidal 17- and 20-ketone groups also proved to be compatible with the oxidizing system.

It is well-known that the C5–C6 double bond of steroids is resistant to BSA. Since blank experiments have shown that the starting olefins do not react with TMSOTf, it can be concluded that a new reactive species is formed in situ (Scheme 1). The most likely candidate is benzeneseleninyl triflate, which is produced in addition to trimethylsilyl benzeneseleninate. The

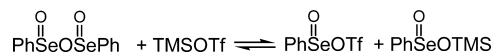
Received: February 21, 2015

Published: May 26, 2015

Table 1. Oxidation of Δ^5 -Steroids with BSA/TMSOTf

Entry	Starting material	Product	Yield
1	 1	 2 ¹⁸	67%
2	 3	 4	80%
3	 5	 6	65%
4	 7	 8 ¹⁹	75%
5	 9	 10 ²⁰	60%
6	 11	 12	87%

Scheme 1. Reaction of BSA with Trimethylsilyl Triflate



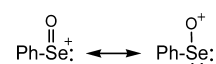
former is probably the active reagent, and the latter serves as a reservoir of oxygen because the transfer of oxygen is possible. Thus, in fact, a 2-fold excess of oxidizing agent was present in the reaction mixture.

It has been previously reported¹⁷ that a similar Se(IV) electrophile (benzeneselenenyl trifluoroacetate) reacts readily with alkenes at room temperature to produce β -trifluoroacetoxy selenoxides that undergo further transformations under the reaction conditions. However, in our case, the product structures may suggest that the double bond is stereoselectively (from the α -side) attacked by the oxygen atom rather than by the selenium atom. In the case of tri- or tetrasubstituted olefins, such an attack would be particularly favorable for steric reasons.

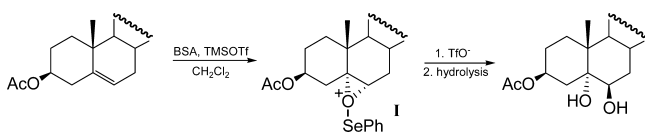
One can assume that the naked benzeneselenenyl cation, which is formed from PhSe(O)OTf in a solvent-stabilizing cation (e.g., dichloromethane), is represented by two mesomeric structures shown below (Scheme 2). However, due to a significant difference in electronegativity between selenium and oxygen atoms, the contribution from the structure on the right would be rather minimal.

Nevertheless, the reaction mechanism shown in Scheme 3 with an oxonium ion I as a key intermediate, which resulted from an attack by the oxygen electrophilic center onto the

Scheme 2. Mesomeric Structures of a Benzeneselenenyl Cation



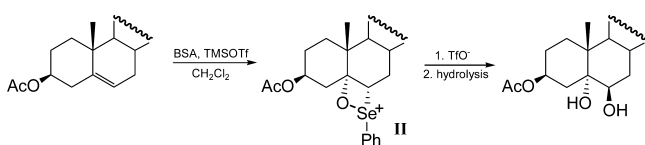
Scheme 3. Tentative Reaction Mechanism via a Three-Membered Cyclic Intermediate



olefin from the α -side, was taken into consideration. The ion I could be cleaved to the *trans*-diol during the aqueous workup of the reaction mixture, or the oxirane ring is first opened with triflate followed by the hydrolysis of a labile diester.

However, there exists an alternative, more likely, reaction mechanism involving formation of a four-membered intermediate II (Scheme 4), which may result from either an initial

Scheme 4. Alternative Reaction Mechanism via a Four-Membered Cyclic Intermediate



electrophilic attack from the α -side of the selenium species onto the olefin followed by cyclization or a concerted [2 + 2] cycloaddition. Then, the selenoxetane ring is opened by a nucleophilic attack of triflate on the carbon atom linked to selenium from the opposite side (S_N2). The two alternative mechanisms will be discussed later within this paper.

The conditions of the oxidation reaction were briefly optimized. The oxidation process was carried out with different amounts of BSA and TMSOTf (from 0.5 up to 1.25 equiv) at various temperatures (from -10°C to rt). The reaction with an excess of BSA and higher contents of TMSOTf afforded lower product yields. The best results were achieved with 1.0 equiv of BSA in the presence of 0.5 equiv of TMSOTf at room temperature as in the first experiments. The optimal reaction time was found to be 45–60 min. When the oxidation of cholesteryl acetate (**1**) was extended to 2 days, the yield of $5\alpha,6\beta$ -diol **2** dropped to 50% and the more oxidized product, 3β -acetoxy- 5α -hydroxycholestan-6-one (43%), appeared. The oxidation of the secondary alcohols to ketones with benzeneseleninic anhydride is a known reaction,² but it is much slower than the reaction of BSA/TMSOTf with olefins.

In the next experiment, the reaction of the tetrasubstituted olefin **13**²¹ was studied (Scheme 5). The reaction proceeded smoothly, affording $10\beta,12\alpha$ -diol **14** in high yield. The structure of compound **14** was confirmed by single-crystal X-ray examination (Figure 1).

The plausible reaction pathway leading to this product is outlined in Scheme 6. It seems that the initial step was analogous to that in the Δ^5 -steroids, that is, the cycloaddition of

Scheme 5. BSA Oxidation of Tetrasubstituted Olefin 13

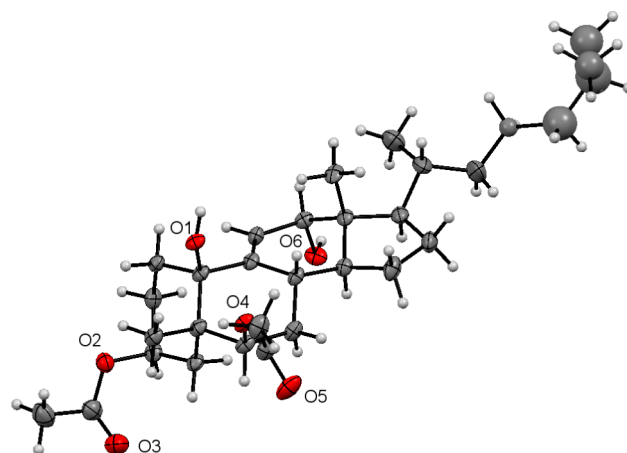
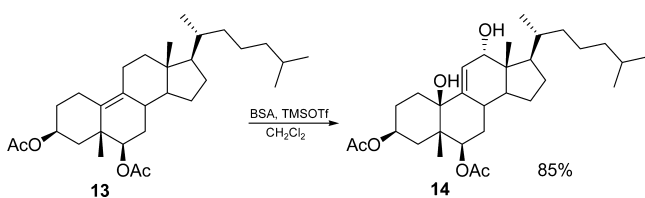


Figure 1. X-ray structure measured at 158 K showing the stereochemistry of compound **14**. Thermal ellipsoids are drawn at the 50% probability level. Disordered *n*-propanol molecule and the side chain with an occupancy of ca. 20% have been omitted for clarity.

the benzeneseleninyl cation to the double bond. The highly hindered olefin **13** reacts with a benzeneseleninyl cation, affording the selenoxetane intermediate **III**. The reaction is highly regio- and stereoselective. In spite of the fact that C10 is more electron-rich than C9 and access to the reagent is easier from the β -side, the calculations (see below) showed that the selenium reagent preferably approaches C9 from the α -side due to the lower energy transition states. In the next step, the selenoxetane intermediate **III** is probably cleaved by a nucleophile (e.g., triflate) with simultaneous elimination of PhSeOH. A different reaction pathway compared to that previously described for analogous intermediate **II** may result from a high steric strain in **III**, which can be released by elimination of PhSeOH. The newly formed C9–C11 double bond undergoes further electrophilic attack by the benzeneseleninyl cation. Further *syn*-elimination of selenoxide afforded the C11–C12 olefin. Finally, the S_N2' addition of an oxygen nucleophile from the less hindered α -side to the olefin at C12, followed by hydrolysis, furnished the final product **14**. The proposed mechanism of C12 hydroxylation of the C9–C11 olefin differs from the usual allylic hydroxylation with the selenium species.²² Alternative reaction mechanisms can also be taken into consideration, including the one with an intramolecular transfer of the benzeneseleninyl cation.

Further study on BSA/TMSOTf oxidation was carried out with exomethylene olefins (Table 2). The reactions of 6- and 12-exomethylene steroids **15** and **17** proved to be much less efficient than the reactions of more hindered olefins. The 6-exomethylene 5α -cholestane derivative **15**, when treated with BSA/TMSOTf, afforded 6-formylcholesteryl acetate **16** in a 40% yield. The analogous reaction of 12-exomethylene tigogenin **17** yielded a mixture of 12ξ -hydroxy-12-formyl derivatives **18a** and **18b** in low yields. The reaction of lupenyl acetate **19** with benzeneseleninic anhydride in the presence of TMSOTf afforded 3β -acetoxy- $20(30)$ -en- 29 -al²³ **20** in a satisfactory yield (75%). The obtained results can be explained by a plausible mechanism shown in Scheme 7. In contrast to the dihydroxylation reactions observed for tri- and tetrasubstituted olefins, in the case of less substituted olefins, the unsaturated aldehydes or α -hydroxyaldehydes were formed. Most likely, an attack of a benzeneseleninyl cation onto the double bond with a soft electrophilic center at selenium

Scheme 6. Tentative Mechanism of the BSA Oxidation of Compound 13

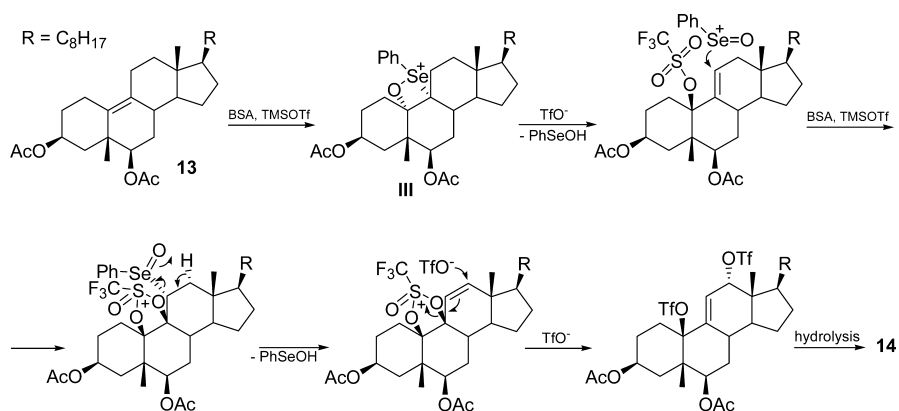


Table 2. Oxidation of 1,1-Disubstituted Olefins with BSA/TMSOTf

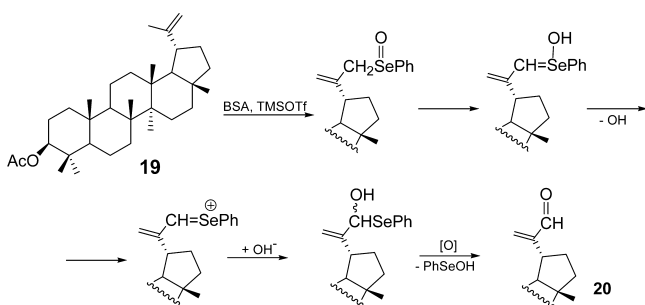
Entry	Starting material	Product	Yield
1	 15	 16	40%
2	 17	 18a 18b	10% 7%
3	 19	 20	75%
4	 21	 22 23	40% 30%

occurred. The carbocation thus-formed may undergo a proton abstraction or an oxygen nucleophile addition. Further oxidation leads to the α,β -unsaturated (e.g., 16 or 20) or α -hydroxy (e.g., 18a or 18b) carbonyl compounds, respectively.

However, a different reaction course was observed for (+)-camphene 21. The initially formed carbocation underwent

various Wagner–Meerwein-type rearrangements (Scheme 8).²⁴ The expected unsaturated aldehyde could not be formed due to the steric hindrance. Two reaction products were formed, but none of them showed the presence of a formyl group. Instead, the oxoselenide 22 and the dioxo compound 23 were obtained as products. The former compound underwent a trans-

Scheme 7. Tentative Reaction Pathway of Lupenyl Acetate 19 with BSA



formation to the latter upon further oxidation and rearrangement. The driving force for this rearrangement is a tendency to assume a bicyclo[2.2.2]octane structure that is less strained than the starting bicyclo[2.2.1]heptane ring system. It should be mentioned that diketone **23** is a known compound,²⁵ and spectral data of the obtained product are consistent with the proposed structure. Of course, compound **23** obtained from **21** was optically active ($[\alpha]_D^{20} +18.2$ (c 0.5, CHCl_3)), unlike the racemic diketone described in the literature. Interestingly, an alternative pathway leading to the symmetrical diketone **24** did not take place.

To provide an insight into the mechanism of the $\text{PhSe}(\text{O})^+$ attack on the olefin double bond, two alternative pathways, leading to four- and three-membered intermediate products, have been studied by quantum-chemical calculations. The calculations were performed at the B3LYP/6-31G**/PCM-(CH_2Cl_2) level by using the Gaussian 09 package of programs (see the Supporting Information for computational details). Such an approach requires, at first, finding the most stable conformers of the interacting systems for the substrates as well as for the products. As the reagents approach each other during the process, they reorganize themselves, weakly bond, and an entrance channel complex (ECC) is formed. To form the products, the system has to overcome an energetic barrier. Estimation of the barrier at a given reaction pathway requires proper identification of the transition state structure (TS).

The first simulated reaction was the $\text{PhSe}(\text{O})^+$ α -side attack on the C5–C6 double bond of model steroid **7** (**M7**), and the corresponding energetic diagram is presented in Figure 2.

Considered reaction paths pass through four- and three-membered TSs (TS-R4 and TS-R3, respectively) and lead to

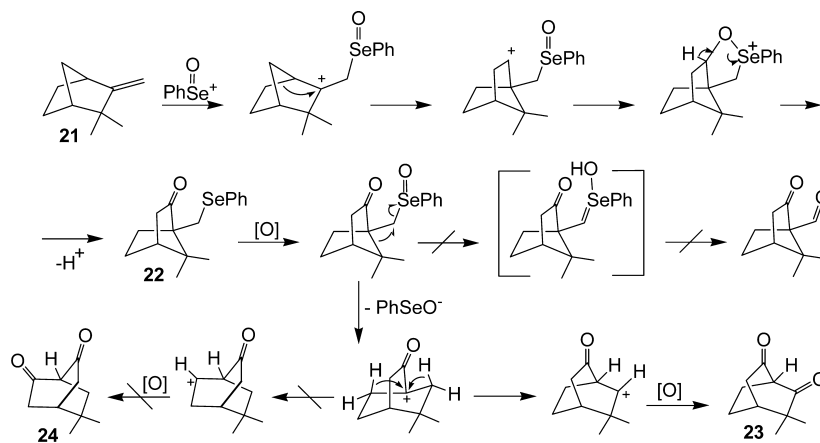
the desired intermediate ions **I** (Scheme 3) and **II** (Scheme 4). In the route leading to **II**, according to Markovnikov's rule, the O atom attack on the positively charged carbon atom was considered only (the NBO analysis of the charge distribution can be seen in Supporting Information Figure S1C). It is a spontaneous reaction; however, a competition between thermodynamic and kinetic reaction control is predicted: the kinetics favors the ${}^{\alpha}\text{R3}$ intermediate product (**I**), while thermodynamics favors the ${}^{\alpha}\text{R4}$ (**II**) one. Moreover, in ion **I**, the $\text{PhSe}(\text{O})^+$ moiety adopts a nonplanar geometry (followed by spectacular changes in the charge distribution within both the $\text{PhSe}(\text{O})^+$ and **M7** moieties in **I**, Table S4P), and the Se–O and Ph–Se distances are longer in comparison to the appropriate distances in the isolated system by ca. 0.3 and 0.02 Å, respectively (Figure S2). Because the difference in stability of ${}^{\alpha}\text{R3}$ and ${}^{\alpha}\text{R4}$ ions is ca. 6 kcal/mol, and the ${}^{\alpha}\text{TS-R4}$ is above ${}^{\alpha}\text{TS-R3}$ by ca. 1.3 kcal/mol, the thermodynamic product **II** dominates under the reaction conditions employed. Moreover, this reaction is a concerted [2 + 2] cycloaddition, yet the process is highly asynchronous: the longer $\sigma(\text{C}–\text{Se})$ bond in ${}^{\alpha}\text{R4}$ is formed earlier in the ${}^{\alpha}\text{TS-R4}$ than is the shorter $\sigma(\text{C}–\text{O})$ one (Figure 2).

Also, the $\text{PhSe}(\text{O})^+$ β -side attack on the C5–C6 double bond of the model **M7** steroid was taken into account. However, as expected, this reaction path is not energetically favored (Supporting Information Diagram S1).

The other studied reaction was the $\text{PhSe}(\text{O})^+$ attack on the olefin double bond of the model reactant **13** (**M13**). In this case, the attacks from both sides (α and β) leading to formation of the four- or three-membered intermediate **III** (R4 or R3 , respectively) and the selenium atom attack on the C9 or C10 atoms were considered. The α -side attack is energetically favored in comparison to the β -attack (Supporting Information Diagram S2) and is presented in Figure 3. For each of the reaction paths, the ECCs and the appropriate TSs via the four-membered ring geometries (TS-R4) were found. Unfortunately, the TSs via the three-membered ring structures (TS-R3) were not found because of convergence problems. All of the considered structures are collected in the Supporting Information Tables S5–S8.

In the preferred reaction path (Figure 3), $\text{PhSe}(\text{O})^+$ approaches **M13** from the α -side: the reaction starts from ECC- ${}^{\alpha}\text{R4}(\text{Se}^{\text{C9}})$, passes through the lowest ${}^{\alpha}\text{TS-R4}(\text{Se}^{\text{C9}})$ activation barrier, and ends up with the most stable intermediate product ${}^{\alpha}\text{R4}(\text{Se}^{\text{C9}})$. Thus, ${}^{\alpha}\text{R4}(\text{Se}^{\text{C9}})$ is both

Scheme 8. Tentative Reaction Pathway of (+)-Camphene 21 with BSA



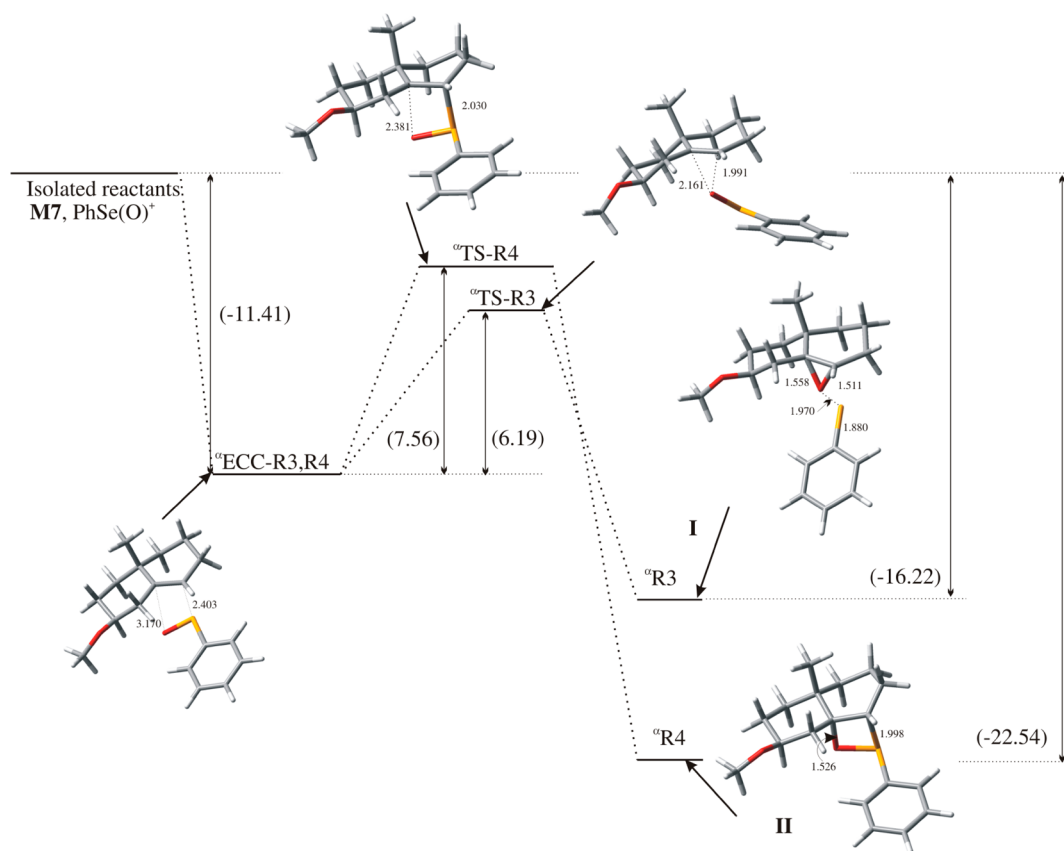


Figure 2. Energetic diagram (in terms of ΔG values, kcal/mol) of $\text{PhSe}(\text{O})^+$ α -attack on the double bond of model olefin **M7** calculated at the B3LYP/6-31G**/PCM(CH_2Cl_2) level. Atoms are color-coded: carbon (gray), hydrogen (white), oxygen (red), and selenium (yellow).

kinetically and thermodynamically the most stable ion. What is surprising, to form ${}^{\alpha}\text{R4}(\text{Se}^{\text{C9}})$, the positively charged Se atom approaches the less negative charged C9 carbon atom of **M13** (Figure S5C). A deeper insight into the charge distribution indicates that, during the process, the electron density is reorganized, and in ${}^{\alpha}\text{TS-R4}(\text{Se}^{\text{C9}})$, it is changed (Table S7D) in comparison to the noninteracting **M13**. In the ${}^{\alpha}\text{TS-R4}(\text{Se}^{\text{C9}})$ structure, the C9 atom becomes more negative (and is more likely to form a bond with the positively charged Se atom) and the C10 atom becomes more positive (and prepared for bond formation with the negatively charged O atom). The stability of the reaction species was additionally checked at two different calculation levels: one accounting for dispersion (B3LYP-D3) and the other by using a basis set incorporating the diffuse functions (6-31+G**, Table S3). The energetic order is not changed; therefore, stability of ${}^{\alpha}\text{R4}(\text{Se}^{\text{C9}})$ is not a computational artifact. Analyzing the geometry and visualizing the imaginary frequency of the ${}^{\alpha}\text{TS-R4}(\text{Se}^{\text{C9}})$ structure, one can conclude that the $\text{PhSe}(\text{O})^+$ α -side attack on the olefin double bond of the model **M13** is a concerted synchronous [2 + 2] cycloaddition (Figure 3).

CONCLUSION

A new and effective, one-pot method for the oxidation of olefins has been reported. The method consists of the generation of a reactive species, presumably the benzeneseleninyl cation, by the treatment of BSA with TMSOTf. In the case of BSA/TMSOTf reactions with simple mono- or disubstituted olefins, the initial step is usually an electrophilic attack of selenium at the less substituted carbon atom. This step

is followed by different consecutive reactions that cause the method to be rather ineffective. However, the BSA/TMSOTf reactions with encumbered tri- and tetrasubstituted olefins proceeded smoothly, affording products in high yields. The dihydroxylated products are formed presumably via the four-membered cyclic intermediate that is formed by a concerted [2 + 2] cycloaddition of a benzeneseleninyl cation to the olefin. The DFT calculations show that such a mechanism is superior to alternative mechanisms.

EXPERIMENTAL SECTION

General Methods. Reagent-grade chemicals were purchased and used as received. The methylene chloride was dried prior to use by distillation over CaH_2 . Flash column chromatography and dry flash chromatography were performed with a silica gel, with a pore size of 40 Å (70–230 mesh), unless otherwise stated. Reactions were monitored by TLC on silica gel plates 60 F₂₅₄. All reactions were carried out under an argon atmosphere. ^1H and ^{13}C NMR data for all previously uncharacterized compounds were recorded at ambient temperature using 400 and 200 MHz spectrometers and are referenced to tetramethylsilane (0.0 ppm) and CDCl_3 (77.0 ppm), respectively, unless otherwise noted. NMR resonance multiplicities are reported using the following abbreviations: br = broad, s = singlet, d = doublet, t = triplet, q = quartet, and m = multiplet; coupling constants, J , are reported in hertz. IR spectral data were obtained using an FT-IR spectrometer (taken in a CHCl_3 solution) and are reported in cm^{-1} . Melting points were determined by a Kofler bench (Böetius type) apparatus and are uncorrected. HR-MS values were obtained on an electrospray ionization time of flight (ESI-TOF) or electron ionization (EI) spectrometers. The specific rotations were acquired on a digital polarimeter.

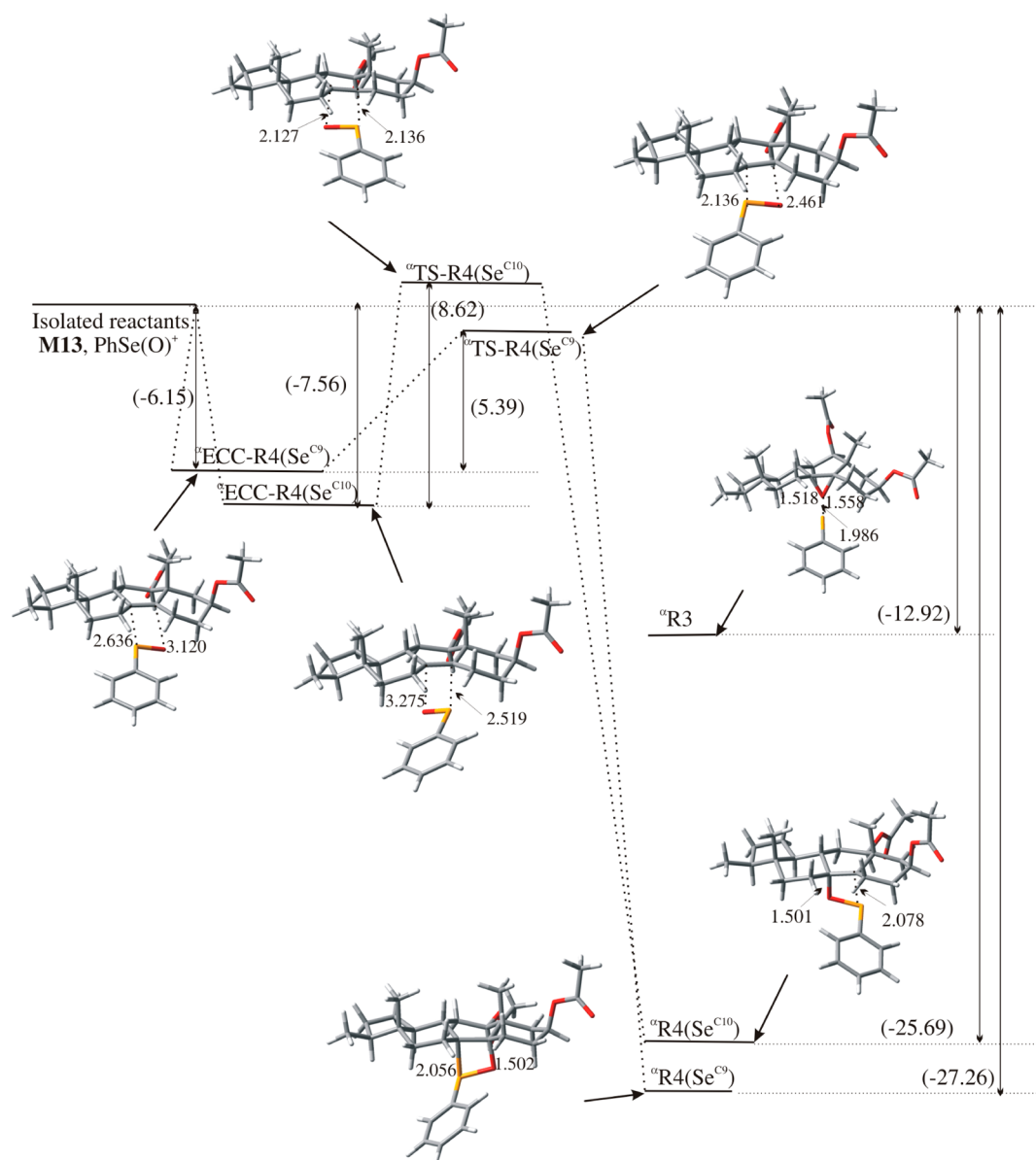


Figure 3. Energetic diagram (in terms of ΔG values, kcal/mol) of $\text{PhSe}(\text{O})^+$ α -attack on the double bond of model olefin **M13** calculated at the B3LYP/6-31G**/PCM(CH_2Cl_2) level. Atoms are color-coded: carbon (gray), hydrogen (white), oxygen (red), and selenium (yellow).

General Experimental Procedure. TMSOTf (0.5 equiv) was added to BSA (1.0 equiv) in dry dichloromethane under argon at room temperature. After 5–10 min of stirring, a solution of alkene (0.2–0.5 mmol) in dry dichloromethane was added. The reaction mixture was stirred under argon. The disappearance of the starting material spot was monitored by TLC. Water was added to the reaction mixture, and then it was extracted with CH_2Cl_2 , dried over MgSO_4 , and evaporated.

5 α ,6 β -Dihydroxycholesterol Acetate (2). The reaction with cholesterol acetate (**1**; 100 mg) was carried out (reaction time = 1 h). Silica gel column chromatography gave pure compound **2** (70 mg; 67%), eluted with 1:1 ethyl acetate/hexane. Compound **2** was proven in all respects to be identical to the same compound described in the literature.¹⁸

5 α ,6 β -Dihydroxycholesterol *p*-Toluenesulfonate (4). The reaction with cholesterol *p*-tosylate (**3**; 108 mg) was carried out (reaction time = 1 h). Silica gel column chromatography gave pure compound **4** (92 mg; 80%) eluted with 17% ethyl acetate in hexane: colorless crystals; mp 149–150 °C (acetone); lit.²⁶ mp 148–150 °C; $^1\text{H NMR}$ δ 7.79 (d, J = 8.2 Hz, 2H), 7.32 (d, J = 8.0 Hz, 2H), 4.93 (m, 1H), 3.50 (br s, 1H), 2.44 (s, 3H), 2.35 (t, J = 11.9 Hz, 1H), 1.97 (d, J

= 12.7 Hz, 1H), 1.14 (s, 3H), 0.90 (s, 3H), 0.89 (s, 3H), 0.86 (dd, J = 6.5, 1.3 Hz, 6H); ESI-MS (m/z , %) 441 ($[\text{MNa}^+ - \text{Ts}^- - \text{H}]^+$, 100). Anal. Calcd for $\text{C}_{34}\text{H}_{54}\text{O}_5\text{S}$: C, 71.04; H, 9.47. Found: C, 70.90; H, 9.49.

(25R)-5 α ,6 β -Dihydroxyspirostan-3 β -ol Acetate (6). The reaction with diosgenin acetate (**5**; 100 mg) was carried out (reaction time = 3 h). Silica gel column chromatography gave pure compound **6** (70 mg; 65%) eluted with 1:1 ethyl acetate/hexane: colorless crystals; mp 256–258 °C (CH_2Cl_2); IR (KBr) ν_{max} (cm^{-1}) 3620, 3461, 1717, 1254; $^1\text{H NMR}$ δ 5.15 (m, 1H), 4.40 (m, 1H), 3.54 (br s, 1H), 3.49 (dd, J = 10.9, 4.6 Hz, 1H), 3.37 (t, J = 10.9 Hz, 1H), 2.18 (t, J = 12.7 Hz, 1H), 2.03 (s, 3H), 1.21 (s, 3H), 0.97 (d, J = 6.7 Hz, 3H), 0.80 (s, 3H), 0.79 (d, J = 6.2 Hz, 6H); $^{13}\text{C NMR}$ δ 171.0 (C), 109.2 (C), 80.7 (CH), 75.9 (CH), 75.5 (C), 71.3 (CH), 66.8 (CH_2), 62.1 (CH), 55.7 (CH), 45.4 (CH), 41.6 (CH), 40.6 (C), 39.9 (CH_2), 38.4 (C), 36.9 (CH_2), 34.8 (CH_2), 32.1 (CH_2), 31.7 (CH_2), 31.3 (CH_2), 30.2 (CH), 29.8 (CH), 28.8 (CH_2), 26.6 (CH_2), 21.4 (CH_3), 20.9 (CH_2), 17.1 (CH_3), 16.6 (CH_3), 16.5 (CH_3), 14.4 (CH_3); ESI-MS (m/z , %) 513 ($[\text{M} + \text{Na}]^+$, 100), 1003 ($[\text{2M} + \text{Na}]^+$, 50). Anal. Calcd for $\text{C}_{29}\text{H}_{46}\text{O}_6$: C, 70.99; H, 9.45. Found: C, 71.11; H, 9.28.

3 β -Acetoxy-5 α ,6 β -dihydroxyandrost-17-one (8). The reaction with androst-5-en-3 β -ol-17-one acetate (**7**; 72 mg) was carried out (reaction time = 1 h). Silica gel column chromatography gave pure compound **8** (60 mg; 75%) eluted with ethyl acetate. Compound **8** was proven in all respects to be identical to the same compound described in the literature.¹⁹

3 β -tert-Butyldimethylsilyloxy-5 α ,6 β -dihydroxypregnan-20-one (10). The reaction with pregn-5-en-3 β -ol-20-one tert-butyldimethylsilyl ether (**9**; 96 mg) was carried out (reaction time = 1 h). Silica gel column chromatography gave pure compound **10** (58 mg; 60%) eluted with 20% ethyl acetate in hexane. Compound **10** was proven in all respects to be identical to the same compound described in the literature.²⁰

3 β ,5 α ,6 β ,21-Tetrahydroxypregnan-20-one 3,21-diacetate (12). The reaction with pregn-5-ene-3 β ,21-diol-20-one 3,21-diacetate (**11**; 82 mg) was carried out (reaction time = 3 h). Silica gel column chromatography gave pure compound **12** (78 mg; 87%) eluted with ethyl acetate: colorless crystals; mp 233–235 °C (CH₂Cl₂); IR (KBr) ν_{\max} (cm⁻¹) 3521, 1750, 1728, 1232; ¹H NMR (CD₃OD) δ 4.72 (d, *J* = 16.8 Hz, 1H), 4.54 (d, *J* = 16.8 Hz, 1H), 4.11 (m, 1H), 3.56 (br s, 1H), 2.52 (t, *J* = 8.8 Hz, 1H), 2.18 (s, 3H), 1.19 (s, 3H), 0.69 (s, 3H); ¹³C NMR (CD₃OD) δ 206.3 (C), 172.0 (C), 76.7 (C), 76.4 (CH), 70.5 (CH₂), 68.3 (CH), 60.3 (CH), 57.7 (CH), 46.4 (CH), 46.1 (C), 41.4 (CH₂), 31.8 (CH₂), 39.4 (C), 33.5 (CH₂), 31.7 (CH), 29.7 (CH₂), 25.5 (CH₂), 23.8 (CH₂), 22.3 (CH₂), 20.3 (CH₂), 17.3 (CH₃), 13.7 (CH₃); ESI-MS (*m/z*, %) 431 ([M + Na]⁺, 100). Anal. Calcd for C₂₅H₃₈O₇: C, 66.64; H, 8.50. Found: C, 66.41; H, 8.63.

5 β -Methyl-19-norcholest-9(11)-ene-3 β ,6 β ,10 β ,12 α -tetraol 3,6-Diacetate (14). The reaction with 5 β -methyl-19-norcholest-9(10)-ene-3 β ,6 β -diol 3,6-diacetate (**13**; 95 mg) was carried out (reaction time = 50 min). Silica gel column chromatography gave pure compound **14** (86 mg, 85%) eluted with 30% ethyl acetate in hexane: colorless crystals; mp 95–96 °C (*n*-propanol/CH₂Cl₂); [α]_D²⁰ –1.5 (c 0.5, CHCl₃); IR (KBr) ν_{\max} (cm⁻¹) 3578, 1732, 1035; ¹H NMR δ 5.97 (d, *J* = 5.6, 1.6 Hz 1H), 5.01 (t, *J* = 3.1 Hz 1H), 4.78 (bs, 1H), 4.03 (d, *J* = 5.6 Hz, 1H), 2.99 (br s, 1H), 2.15 (s, 3H), 2.04 (s, 3H), 0.99 (d, *J* = 6.6 Hz, 3H), 0.87 (2d, *J* = 6.6 Hz, 3H), 0.64 (s, 3H); ¹³C NMR δ 170.2 (C), 169.5 (C), 141.9 (C), 124.6 (CH), 74.5 (C), 72.0 (CH), 68.8 (CH), 47.2 (CH), 45.7 (CH), 44.8 (C), 41.2 (C), 39.4 (CH₂ x 2), 36.2 (CH₂), 35.9 (CH₂), 35.3 (CH), 31.4 (CH), 31.2 (CH₂), 27.9 (CH x 2), 27.7 (CH₂ x 2), 24.7 (CH₂), 23.8 (CH₂), 22.7 (CH₃), 22.5 (CH₃), 21.4 (CH₃), 21.2 (CH₂), 18.8 (CH₃), 17.5 (CH₃), 11.2 (CH₃); ESI-MS (*m/z*, %) 541 ([M + Na]⁺, 100); HRMS (ESI TOF) *m/z* [M + Na]⁺ calcd for C₃₁H₅₀O₆Na 541.3505; found 541.3492.

X-ray Structure Determination. C₃₁H₄₆O₆, C₃H₈O, MW = 577.79, orthorhombic space group P2₁2₁2, *a* = 17.1991(6), *b* = 32.357(1), *c* = 5.9359(2) Å, *V* = 3303.4(2) Å³, *F*(000) = 1268, *d*_{calc} = 1.162 Mg m⁻³, *Z* = 4, *m*(Cu K α) = 0.632 cm⁻¹, *T* = 158 K, crystal size 0.421 × 0.165 × 0.107 mm, 30 264 reflections measured and corrected for numerical absorption with *T*_{min} = 0.777 and *T*_{max} = 0.935, 5976 reflections were unique (*R*_{int} = 0.0525), final *R*₁ = 0.0576, *wR*₂ = 0.1600, for 5557 observed reflections with [*I* > 2 σ (*I*)]; GOF = 1.040. Absolute structure (Flack) parameter 0.1(3).

Intensity data for the single crystals were obtained by collecting reflections at 158 K using 0.5° ω scans on a Bruker X8 diffractometer furnished with an APEX II CCD detector using Cu K α (λ = 1.54178 Å) radiation. Aliphatic group hydrogen atoms were placed at their idealized positions and allowed to ride on the coordinates of the parent atom with isotropic thermal parameters (*U*_{iso}) fixed at 1.2 *U*_{eq} of the carbon atom to which they are attached. Hydroxyl group hydrogens were found from the difference electron density maps and refined with an anisotropic thermal motion model.

Crystallographic data have been deposited at the Cambridge Crystallographic Data Centre, 12 Union Road, 129 Cambridge CB2 1EZ, UK, and copies can be obtained on request, free of charge, by quoting the publication citation and the deposition number CCDC 1047802.

6-Formylcholest-5-en-3 β -ol acetate (16). The reaction with 6-methylene-5 α -cholestan-3 β -ol acetate (**15**; 80 mg) was carried out (reaction time = 45 min). Silica gel column chromatography gave pure

compound **16** as an oil (32 mg; 40%) eluted with 10% ethyl acetate in hexane: colorless oil; IR (KBr) ν_{\max} (cm⁻¹) 1728, 1662, 1250; ¹H NMR δ 10.19 (s, 1H), 4.70 (m, 1H), 3.70 (ddd, *J* = 13.9, 4.4, 1.8 Hz, 1H), 2.49 (ddd, *J* = 17.8, 5.0, 2.8 Hz, 1H), 2.07 (s, 3H), 1.16 (s, 3H), 0.88 (d, *J* = 1.8 Hz, 3H), 0.86 (d, *J* = 1.8 Hz, 3H), 0.69 (s, 3H); ¹³C NMR δ 191.0 (CH), 170.3 (C), 159.1 (C), 133.7 (C), 73.0 (CH), 56.6 (CH), 56.1 (CH), 49.3 (CH), 42.2 (C), 39.5 (CH₂), 39.4 (CH₂), 38.9 (C), 36.3 (CH₂), 36.1 (CH₂), 35.8 (CH), 30.6 (CH), 29.7 (CH₂), 29.6 (CH₂), 28.2 (CH₂), 28.0 (CH), 27.1 (CH₂), 24.2 (CH₂), 23.8 (CH₂), 22.8 (CH₃), 22.5 (CH₃), 21.3 (CH₃), 21.1 (CH₂), 19.8 (CH₃), 18.7 (CH₃), 11.8 (CH₃); ESI-MS (*m/z*, %) 479 ([M + Na]⁺, 100). Anal. Calcd for C₃₀H₄₈O₃: C, 78.90; H, 10.59. Found: C, 78.66; H, 10.69.

(25R)-12-Formyl-5 α -spirostane-3 β ,12 ξ -diol 3-Acetate (18a and 18b). The reaction with (25R)-12-methylene-5 α -spirostan-3 β -ol acetate (**17**; 100 mg) was carried out (reaction time = 40 min). Silica gel column chromatography gave compound **18a** (10 mg; 10%) followed by the more polar **18b** (7 mg, 7%) eluted with 10% ethyl acetate in hexane. **18a** (amorphous solid): IR (KBr) ν_{\max} (cm⁻¹) 3494, 1715, 1256, 1049; ¹H NMR δ 10.16 (d, *J* = 1.0 Hz, 1H), 4.68 (m, 1H), 4.37 (m, 1H), 3.52 (d, *J* = 1.0 Hz, 1H), 3.45 (ddd, *J* = 11.0, 4.4, 2.0 Hz, 1H), 3.33 (t, *J* = 11.0 Hz, 1H), 2.02 (s, 3H), 1.01 (s, 3H), 0.90 (d, *J* = 6.9 Hz, 3H), 0.88 (s, 3H), 0.78 (d, *J* = 6.3 Hz, 3H); ¹³C NMR δ 206.1 (CH), 170.6 (C), 109.5 (C), 80.9 (C), 79.8 (CH), 73.2 (CH), 66.9 (CH₂), 57.6 (CH), 52.6 (CH), 51.5 (CH), 48.0 (C), 44.7 (CH), 42.2 (CH), 36.6 (CH₂), 35.9 (C), 34.6 (CH), 33.8 (CH₂), 32.9 (CH₂), 31.7 (CH₂), 31.3 (CH₂), 31.0 (CH₂), 30.2 (CH), 28.7 (CH₂), 28.3 (CH₂), 27.3 (CH₂), 21.4 (CH₃), 17.1 (CH₃), 13.3 (CH₃), 12.5 (CH₃), 11.5 (CH₃); ESI-MS (*m/z*, %) 525 ([M + Na]⁺, 100). Anal. Calcd for C₃₀H₄₆O₆: C, 71.68; H, 9.22. Found: C, 71.45; H, 9.33. **18b** (amorphous solid): IR (KBr) ν_{\max} (cm⁻¹) 3505, 1716, 1256, 1051; ¹H NMR δ 9.77 (d, *J* = 1.0 Hz, 1H), 4.68 (m, 1H), 4.39 (m, 1H), 3.47 (ddd, *J* = 11.0, 4.2, 2.0 Hz, 1H), 3.34 (t, *J* = 11.0 Hz, 1H), 3.32 (d, *J* = 1.0 Hz, 1H), 2.02 (s, 3H), 1.08 (s, 3H), 0.91 (s, 3H), 0.79 (d, *J* = 7.0 Hz, 3H), 0.78 (d, *J* = 6.3 Hz, 3H); ¹³C NMR δ 205.1 (CH), 170.6 (C), 108.9 (C), 80.2 (CH), 79.9 (C), 73.4 (CH), 66.9 (CH₂), 52.7 (CH), 49.8 (CH), 48.1 (CH), 47.6 (C), 44.5 (CH), 41.9 (CH), 36.4 (CH₂), 35.3 (C), 34.8 (CH), 33.9 (CH₂), 31.6 (CH₂), 31.5 (CH₂), 30.4 (CH₂), 30.2 (CH), 28.8 (CH₂), 28.4 (CH₂), 28.1 (CH₂), 27.3 (CH₂), 21.4 (CH₃), 17.1 (CH₃), 14.3 (CH₃), 13.8 (CH₃), 12.1 (CH₃); ESI-MS (*m/z*, %) 525 ([M + Na]⁺, 100). Anal. Calcd for C₃₀H₄₆O₆: C, 71.68; H, 9.22. Found: C, 71.49; H, 9.29.

3 β -Acetoxyilup-20(30)-en-29-ol (20). The reaction with lupeol acetate (**19**; 94 mg) was carried out (reaction time = 50 min). Silica gel column chromatography gave pure compound **7** (72 mg; 75%) eluted with 5% ethyl acetate/hexane. Compound **7A** was proven in all respects to be identical to the same compound described in the literature.²⁴

2,2-Dimethylbicyclo[2,2,1]-1-phenylselenomethylheptan-5-one (22) and 3,3-Dimethylbicyclo[2,2,2]octan-2,6-dione (23). The reaction with (+)-camphene (**21**; 75 mg) was carried out (reaction time = 1.5 h). Silica gel column chromatography gave pure compound **22** as a yellow oil (68 mg; 40%) and compound **23** as an amorphous solid (27 mg, 30%) eluted with 5 and 7% ethyl acetate in hexane, respectively. **22**: IR (KBr) ν_{\max} (cm⁻¹) 1709, 1579, 1478; ¹H NMR δ 7.52 (m, 2H), 7.23 (m, 3H), 3.84 (s, 1H), 2.93 (t, *J* = 5.1 Hz, 1H), 2.16 (d, *J* = 12.6 Hz, 1H), 2.08 (t, *J* = 5.1 Hz, 1H), 2.01 (m, 2H), 1.85 (2H), 1.23 (s, 3H), 1.01 (s, 3H); ¹³C NMR δ 208.7 (C), 133.7 (CH), 131.2 (C), 129.0 (CH x 2), 127.1 (CH), 64.6 (CH), 50.5 (CH), 47.8 (CH), 44.2 (C), 34.7 (CH₂), 27.7 (CH₃), 27.2 (CH₂ x 2), 24.7 (CH₂), 24.3 (CH₃); ESI-MS (*m/z*, %) 331 ([M + Na]⁺, 100), 639 ([2M + Na]⁺, 100). Anal. Calcd for C₁₆H₂₀OSe: C, 62.54; H, 6.56. Found: C, 62.31; H, 6.39. **23**: [α]_D²⁰ +18.2 (c 0.5, CHCl₃); IR (KBr) ν_{\max} (cm⁻¹) 1728, 1717, 1463; ¹H NMR δ 3.13 (q, *J* = 6.3, 0.6 Hz, 1H), 2.43 (d, *J* = 13.2 Hz, 1H), 2.21 (d, *J* = 5.3 Hz, 1H), 2.07 (m, 1H), 1.88 (3H), 1.63 (m, 1H), 1.23 (s, 3H), 1.16 (s, 3H); ¹³C NMR δ 205.2 (C), 200.0 (C), 51.4 (C), 51.0 (CH), 47.0 (CH), 33.5 (CH₂), 25.5 (CH₂), 24.6 (CH₂), 24.5 (CH₃), 21.8 (CH₃); ESI-MS (*m/z*, %) 221 ([M + Na + MeOH]⁺, 100), 189 ([M + Na]⁺, 100). Anal. Calcd for C₁₀H₁₄O₂: C, 72.26; H, 8.49. Found: C, 72.01; H, 8.35.

Calculations. The hybrid Becke three-parameter Lee–Yang–Parr density functional theory (DFT) B3LYP functional^{27,28} and 6-31G** basis set²⁹ were applied in this study. This computational level provides an acceptable compromise between computational labor and basis set error. The first step of the calculations was conformational analysis performed by the Conflex program,^{30–32} in which the MMFF94s force field was implemented. For the reaction modeling, only the most abundant conformers of the reactants were taken for further calculations of the reaction paths. All stationary points (minima and transition structures) were characterized by calculating the harmonic vibrational frequencies, using analytical second derivatives. The transition structures were found by using the quadratic synchronous transit-guided quasi-Newton (QST3) method developed by Schlegel and co-workers.³³ For the lowest reaction barriers of the model M7 reaction, the intrinsic reaction coordinate calculations^{34,35} were performed for both forward and reverse directions of the vibrational mode calculations to confirm that the transition states that were found connect the appropriate minima.

To account for the dichloromethane solvent effect, the polarizable continuum model (PCM) was applied.^{36,37} In this procedure, the solvent is mimicked by a dielectric continuum with a dielectric constant ($\epsilon = 8.93$ for CH_2Cl_2), surrounding a cavity with a shape and dimension adjusted on the real geometric structure of the solute molecule. The latter polarizes the solvent, which, as a response, induces an electric field (the reaction field) that interacts with the solute. In the IEF-PCM, the electrostatic part of such an interaction is represented in terms of an apparent charge density spread on the cavity surface.

The natural bond analysis (NBO)³⁸ was performed to estimate the charge distribution. In this method, natural atomic orbitals that are the effective orbitals of an atom in the particular molecular environment are determined, and these are also the maximum occupancy orbitals. NBOs are localized few-center molecular orbitals that reflect Lewis-like bonding structures.

All of the calculations were performed using the Gaussian 09 package of programs,³⁹ and the structures were visualized by using the GaussView program.⁴⁰

■ ASSOCIATED CONTENT

● Supporting Information

Physical and spectroscopic data for compounds **4**, **6**, **12**, **14**, **16**, **18a**, **18b**, **22**, **23**, **26**, and **27**, and crystallographic information file (CIF) for compound **14**. Computational details (energetics, NBO charges, Cartesian coordinates, the imaginary frequencies assignment) for computed structures. The Supporting Information is available free of charge on the ACS Publications website at DOI: 10.1021/acs.joc.5b00410.

■ AUTHOR INFORMATION

Corresponding Authors

*Tel.: +48 85 7388043. Fax: +48 85 7388103. E-mail: gierdas@uwb.edu.pl.

*Tel.: +48 85 7388260. Fax: +48 85 7388103. E-mail: morzycki@uwb.edu.pl.

Notes

The authors declare no competing financial interest.

■ ACKNOWLEDGMENTS

Financial support from the University of Białystok within the project BST-124 is gratefully acknowledged. The equipment (i.e., digital polarimeter) for the Center of Synthesis and Analysis BioNanoTechno of the University of Białystok was funded by EU, as a part of the Operational Program Development of Eastern Poland 2007–2013, project POPW.01.03.00-20-034/09-00. Computational Grant No. G19-4 from Interdisciplinary Centre for Mathematical and

Computational Modelling of University of Warsaw (ICM) is acknowledged for the computer time. This research was also supported by PL-Grid Infrastructure. We also thank Mrs. Jadwiga Maj for her skillful technical assistance.

■ REFERENCES

- (1) Wirth, T., Ed. *Organoselenium Chemistry*; Wiley-VCH Verlag GmbH & Co.KGaA: Weinheim, Germany, 2012.
- (2) Barton, D. H. R.; Brewster, A. G.; Hui, R. A. H. F.; Lester, D. J.; Ley, S. V. *Chem. Commun.* **1978**, 952–954.
- (3) Barton, D. H. R.; Mangust, P. D.; Rosenfeld, M. N. *Chem. Commun.* **1975**, 301–302.
- (4) Barton, D. H. R.; Brewster, A. G.; Ley, S. V.; Rosenfeld, M. N. *Chem. Commun.* **1976**, 985–986.
- (5) Barton, D. H. R.; Cussano, N. J.; Ley, S. V. *Chem. Commun.* **1978**, 393–394.
- (6) Barton, D. H. R.; Lester, D. J.; Ley, S. V. *Chem. Commun.* **1978**, 276–277.
- (7) Barton, D. H. R.; Lester, D. J.; Ley, S. V. *Chem. Commun.* **1977**, 445–446.
- (8) Back, T. G.; Collins, S.; Kerr, R. G. *J. Org. Chem.* **1981**, *46*, 1564–1570.
- (9) (a) Barton, D. H. R.; Lester, D. J.; Ley, S. V. *Chem. Commun.* **1978**, 130–131. (b) Barton, D. H. R.; Lester, D. J.; Ley, S. V. *J. Chem. Soc., Perkin Trans. 1* **1980**, 2209–2212.
- (10) Back, T. G. *J. Org. Chem.* **1981**, *46*, 1442–446.
- (11) Danieli, B.; Lesma, G.; Palmisano, G.; Riva, E. *Chem. Commun.* **1984**, 909–911.
- (12) (a) Shimizu, M.; Kuwajima, I. *Tetrahedron Lett.* **1979**, *20*, 2801–2804. (b) Kuwajima, I.; Shimizu, M.; Urale, H. *J. Org. Chem.* **1982**, *47*, 837–842.
- (13) (a) Barton, D. H. R.; Morzycki, J. W.; Motherwell, W. B.; Ley, S. V. *Chem. Commun.* **1981**, 1044–1045. (b) Barton, D. H. R.; Godfrey, C. R. A.; Morzycki, J. W.; Motherwell, W. B.; Ley, S. V. *J. Chem. Soc., Perkin Trans. 1* **1982**, 1947–1952. (c) Barton, D. H. R.; Crich, D. *Tetrahedron* **1985**, *41*, 4359–4364.
- (14) ten Brink, G.-J.; Vis, J.-M.; Arends, I. W. C. E.; Sheldon, R. A. *J. Org. Chem.* **2001**, *66*, 2429–2433.
- (15) Ayrey, G.; Barnard, D.; Woodbridge, D. T. *J. Chem. Soc.* **1962**, 2089–2099.
- (16) Kutateladze, A. G.; Kice, J. L.; Kutateladze, T. G.; Zefirov, N. S.; Zyk, N. V. *Tetrahedron Lett.* **1992**, *33*, 1949–1952.
- (17) Kutateladze, A. G.; Kice, J. L.; Kutateladze, T. G.; Zefirov, N. S. *J. Org. Chem.* **1993**, *58*, 995–996.
- (18) Carvalho, J. F. S.; Cruz Silva, M. M.; Sá e Melo, M. L. *Tetrahedron* **2010**, *66*, 2455–2462.
- (19) Ruddock, P. L.; Williams, D. J.; Reese, P. B. *Steroids* **2004**, *69*, 193–199.
- (20) Duran, F. J.; Ghini, A. A.; Coirini, H.; Burton, G. *Tetrahedron* **2006**, *62*, 4762–4768.
- (21) Petrow, V. A. *J. Chem. Soc.* **1939**, 998–1003.
- (22) López, Y.; Jastrzębska, I.; Santillan, R.; Morzycki, J. W. *Steroids* **2008**, *73*, 449–457.
- (23) (a) Ogawa, S.; Hosoi, K.; Makino, M.; Fujimoto, Y.; Iida, T. *Chem. Pharm. Bull.* **2007**, *55*, 247–250. (b) Heisi, K.; Ogawa, S.; Makino, M.; Mukaiyama, T.; Hori, K.; Iida, T.; Fujimoto, Y. *J. Nat. Med.* **2008**, *62*, 332–335.
- (24) Banthrophe, D. V.; Whittaker, D. Q. *Rev. Chem. Soc.* **1966**, *20*, 373–387.
- (25) (a) Spreitzer, H. *Monatsh. Chem.* **1990**, *121*, 847–851. (b) Spreitzer, H.; Buchbauer, G.; Reisinger, S. *Helv. Chim. Acta* **1989**, *72*, 806–810.
- (26) Witiak, D. T.; Parker, R. A.; Dempsy, M. E.; Ritter, M. C. *J. Med. Chem.* **1971**, *14*, 684–693.
- (27) Becke, A. D. *J. Chem. Phys.* **1993**, *98*, 5648–5652.
- (28) Burke, K.; Perdew, J. P.; Wang, Y. *Electronic Density Functional Theory: Recent Progress and New Directions*; Dobson, J. F., Vignale, G., Das, M. P., Eds.; Plenum Press: New York, 1998.

- (29) Rassolov, V. A.; Ratner, M. A.; Pople, J. A.; Redfern, P. C.; Curtiss, L. A. *J. Comput. Chem.* **2001**, *22*, 976–984.
- (30) CONFLEX 7; Conflex Corp.: Japan, 2012.
- (31) Goto, H.; Osawa, E. *J. Am. Chem. Soc.* **1989**, *111*, 8950–8951.
- (32) Goto, H.; Osawa, E. *J. Chem. Soc., Perkin Trans. 2* **1993**, 187–198.
- (33) Peng, C.; Schlegel, H. B. *Isr. J. Chem.* **1993**, *33*, 449–454.
- (34) Gonzales, C.; Schlegel, H. B. *J. Chem. Phys.* **1989**, *90*, 2154–2161.
- (35) Gonzales, C.; Schlegel, H. B. *J. Phys. Chem.* **1990**, *94*, 5523–5527.
- (36) Mennucci, B. *Wiley Interdiscip. Rev.: Comput. Mol. Sci.* **2012**, *2*, 386–404.
- (37) Scalmani, G.; Frisch, M. J. *J. Chem. Phys.* **2010**, *132*, 114110.
- (38) Weinhold, F.; Landis, C. R. *Discovering Chemistry with Natural Bond Orbitals*; John Wiley & Sons: Hoboken, NJ, 2012.
- (39) Frisch, M. J.; Trucks, G. W.; Schlegel, H. B.; Scuseria, G. E.; Robb, M. A.; Cheeseman, J. R.; Scalmani, G.; Barone, V.; Mennucci, B.; Petersson, G. A. et al. *Gaussian 09*, revision A.1; Gaussian, Inc.: Wallingford, CT, 2009.
- (40) Dennington, R.; Keith, T.; Millam, J. *GaussView*, version 5; Semichem Inc.: Shawnee Mission, KS, 2009.